

RESEARCH

Open Access



# Impaired liver regeneration and lipid homeostasis in CCl<sub>4</sub> treated WDR13 deficient mice

Arun Prakash Mishra<sup>\*</sup> , Archana B. Siva, Chandrashekarun Gurunathan, Y. Komala and B. Jyothi Lakshmi

## Abstract

WDR13 - a WD repeat protein, is abundant in pancreas, liver, ovary and testis. Absence of this protein in mice has been seen to be associated with pancreatic  $\beta$ -cell proliferation, hyperinsulinemia and age dependent mild obesity. Previously, we have reported that the absence of WDR13 in diabetic *Lepr<sup>db/db</sup>* mice helps in amelioration of fatty liver phenotype along with diabetes and systemic inflammation. This intrigued us to study direct liver injury and hepatic regeneration in *Wdr13<sup>-/-</sup>* mice using hepatotoxin CCl<sub>4</sub>. In the present study we report slower hepatic regeneration in *Wdr13<sup>-/-</sup>* mice as compared to their wild type littermates after CCl<sub>4</sub> administration. Interestingly, during the regeneration phase, hepatic hypertriglyceridemia was observed in *Wdr13<sup>-/-</sup>* mice. Further analyses revealed an upregulation of PPAR pathway in the liver of CCl<sub>4</sub>- administered *Wdr13<sup>-/-</sup>* mice, causing de novo lipogenesis. The slower hepatic regeneration observed in CCl<sub>4</sub> administered *Wdr13<sup>-/-</sup>* mice, may be linked to liver hypertriglyceridemia because of activation of PPAR pathway.

**Keywords:** Fatty liver, PPAR $\gamma$ , Hepatosteatorosis, Hypertriglyceridemia, Hepatotoxin

## Introduction

Liver is a vital organ responsible for several metabolic processes and over 1 million deaths worldwide were reported from liver cirrhosis in 2010 [1]. Several factors cause liver damage, of which chronic alcohol abuse and viral hepatitis are identified as the major ones [1]. Liver, being one of the fastest regenerating organs [2], rectifies the damage and, in the repair process accumulates extracellular matrix (collagen) resulting in fibrosis [3] causing morphologically and functionally damaged liver [3]. Liver damage also occurs as a result of extensive lipid accumulation - popularly known as fatty liver, that is caused by either high fat diet intake or obesity-associated insulin resistance [non-alcohol dependent steatohepatitis or NASH] [4]. Hepatocyte damage induced by fatty liver condition leads to inflammation and fibrosis in liver [3].

To study liver damage in mouse model, chronic CCl<sub>4</sub> (carbon tetrachloride) administration is an established method [5]. CCl<sub>4</sub> gets metabolized to CCl<sub>3</sub>OO<sup>\*</sup> peroxide free radicals in the liver via mitochondrial cytochrome P450 (CYP450) and the generated peroxide free radicals damage the hepatocyte lipid biomembrane, through lipid peroxidation, resulting in the release of cellular contents in extracellular matrix, eliciting a myriad of inflammatory signals in liver. High level of inflammation leads to apoptosis and further liver damage [6]. These damages are, however, spontaneously reversible if the mice are given a regeneration period of 20 days [7].

WDR13, a member of the WD repeat protein family, is present in most of the mouse tissues, with relatively higher abundance in pancreas, liver, testis and ovary [8]. Previous studies have shown that *Wdr13<sup>-/-</sup>* mice have age-dependent mild obesity, enhanced pancreatic  $\beta$ -cell proliferation, hyperinsulinemia and better glucose clearance [9, 10]. We have also demonstrated that the

\* Correspondence: [apmccmb@gmail.com](mailto:apmccmb@gmail.com)

CSIR- Centre for Cellular and Molecular Biology, Hyderabad 500007, India



© The Author(s). 2020 **Open Access** This article is licensed under a Creative Commons Attribution 4.0 International License, which permits use, sharing, adaptation, distribution and reproduction in any medium or format, as long as you give appropriate credit to the original author(s) and the source, provide a link to the Creative Commons licence, and indicate if changes were made. The images or other third party material in this article are included in the article's Creative Commons licence, unless indicated otherwise in a credit line to the material. If material is not included in the article's Creative Commons licence and your intended use is not permitted by statutory regulation or exceeds the permitted use, you will need to obtain permission directly from the copyright holder. To view a copy of this licence, visit <http://creativecommons.org/licenses/by/4.0/>. The Creative Commons Public Domain Dedication waiver (<http://creativecommons.org/publicdomain/zero/1.0/>) applies to the data made available in this article, unless otherwise stated in a credit line to the data.

introgression of *Wdr13*-null mutation in obese and diabetic *Lep<sup>db/db</sup>* mouse model resulted in reduction of serum free-fatty acids, liver triglyceride and systemic inflammation [11]. Amelioration of fatty liver and cell proliferative phenotype in pancreas, prompted us to study the response of *Wdr13*<sup>-/-</sup> mice to direct liver injury induced by chronic CCl<sub>4</sub> administration and regeneration therein. Slower regeneration and hypertriglyceridemia were observed in the liver of *Wdr13*<sup>-/-</sup> liver after CCl<sub>4</sub> toxicity during the regeneration process when compared to that in their wild type counterparts. The results suggests an association between liver lipid accumulation and regeneration.

## Results

### Effect of *Wdr13* deletion on liver pathology and regeneration after CCl<sub>4</sub> administration

CCl<sub>4</sub> damages the plasma membranes of hepatocytes, which leads to increase in serum glutamic-oxaloacetic transaminase (SGOT) and serum glutamate-pyruvate transaminase (SGPT) levels [12]. The initial damage consequently elicits huge inflammatory response causing severe hepatic damage [12]. To analyse the damage caused by chronic CCl<sub>4</sub> administration, we studied the liver damage parameters, namely; SGOT & SGPT, hepatocytes morphology, collagen deposition, lipid peroxidation and inflammation in WDR13 deficient mice. The mutant mice did not differ significantly from the wild type counterparts in all the above parameters (Supplementary figure). The liver/body weight ratio in *Wdr13*<sup>-/-</sup> mice was found to be lower than that in *Wdr13*<sup>+/-</sup> mice (Fig. 1c). The mutant mice had lower number of actively dividing hepatocytes, as revealed by Ki-67 immunostaining of the liver sections (Fig. 1a,b), indicating that the liver of *Wdr13*<sup>-/-</sup> mice has slower regeneration. To further understand the reason for slow regeneration of *Wdr13*<sup>-/-</sup> livers, we analysed the expression level of cell cycle genes. Lower protein levels of Cyclin D1 and Cyclin E, key molecules for cell cycle G1/S transition, and higher protein level of p53 (anti-proliferative gene) were observed in the liver of *Wdr13*<sup>-/-</sup> mice (Fig. 1d,e).

### Effect of *Wdr13* deletion on liver lipid content after CCl<sub>4</sub> administration

Since our previous study [11] indicated amelioration of fatty liver phenotype upon deletion of *Wdr13* in *Lep<sup>db/db</sup>* mice, we analysed liver triglyceride levels in the present study. In contrast to our earlier study, we observed higher triglycerides level in the liver of CCl<sub>4</sub> administered *Wdr13*<sup>-/-</sup> mice as compared to that in CCl<sub>4</sub> treated wildtypes (Fig. 2b). This observation was further confirmed by Oil Red O staining, which revealed extensive deposition of lipid droplets in the liver of CCl<sub>4</sub> administered *Wdr13*<sup>-/-</sup> mice (Fig. 2a). Substantiating the

above results, relative mRNA levels of lipogenic genes (*Acc1*, *Dgat2*, *Fasn*, and *Srebp1*) were also found to be upregulated in the liver of CCl<sub>4</sub> administered *Wdr13*<sup>-/-</sup> mice (Fig. 2c).

### Analyses of lipid metabolic pathway in *Wdr13* deficient mice on CCl<sub>4</sub> administration

It is known that the Peroxisome proliferator-activated receptor (PPAR) pathway plays a crucial role in lipid metabolism in liver [13] and its upregulation increases lipid accumulation therein [14–18]. We analysed the PPAR pathway proteins- PPAR $\gamma$ , P-p38 $\alpha$ , p38 $\alpha$ , and Adenylyl Cyclase 1 (AC1), by western blot analyses and observed higher levels of each of these proteins in the liver of CCl<sub>4</sub> administered *Wdr13*<sup>-/-</sup> mice (Fig. 3a, b). Additionally, the relative mRNA levels of *Ppar $\gamma$*  and *Ppara*, in the liver of CCl<sub>4</sub> administered *Wdr13*<sup>-/-</sup> mice, were also found to be upregulated (Fig. 3c). The downstream target genes (Fig. 3d) of PPAR $\alpha$  & PPAR $\gamma$  (*Adipoq*, *Ap2*, *Cpt1* and *CD36*) and the upstream genes to the PPAR pathway (Fig. 3c) - *Prkaca1* (catalytic subunit of protein kinase A), *p38 $\alpha$*  & adenylyl cyclase 1 (*Ac1*) were all up-regulated, confirming higher activity of PPARs in the liver of CCl<sub>4</sub> administered *Wdr13*<sup>-/-</sup> mice via the p38 $\alpha$ /MAPK14 and PKA pathway. This upregulation of PPAR pathway in CCl<sub>4</sub> treated *Wdr13*<sup>-/-</sup> livers leads to the de novo lipogenesis and accumulation of triglycerides therein.

### CCl<sub>4</sub> toxicity on primary hepatocytes

The mouse model under the present study is a whole body *Wdr13* gene knockout, and therefore, the observed phenotype may have resulted because of the systemic absence of WDR13. To understand if the observed phenotype was indeed due to the absence of WDR13 in liver, we performed experiments with primary hepatocytes from *Wdr13*<sup>+/-</sup> and *Wdr13*<sup>-/-</sup> mice. CCl<sub>4</sub> toxicity on primary hepatocytes was analysed by culturing the isolated hepatocytes with increasing concentration of CCl<sub>4</sub> (0.0–0.25 mM). MTT assay revealed that *Wdr13*<sup>-/-</sup> hepatocytes are more susceptible to CCl<sub>4</sub> (Fig. 4a), as seen by reduced cell viability at even the lowest concentration of CCl<sub>4</sub> (0.05 mM).

To analyse the genes in the PPAR pathway in primary hepatocytes, *Wdr13*<sup>+/-</sup> and *Wdr13*<sup>-/-</sup> hepatocytes were treated with 0.1 M CCl<sub>4</sub> for 24 h and then harvested for total RNA isolation and qPCR. Consistent with the in vivo results, the qPCR analysis of cDNA from CCl<sub>4</sub> treated hepatocytes indicated upregulation of the PPAR pathway along with the upstream genes- *Ac1* & *p38 $\alpha$*  and other lipid metabolism genes (*Acc1* & *Dgat2*) in *Wdr13*<sup>-/-</sup> hepatocytes (Fig. 4b).

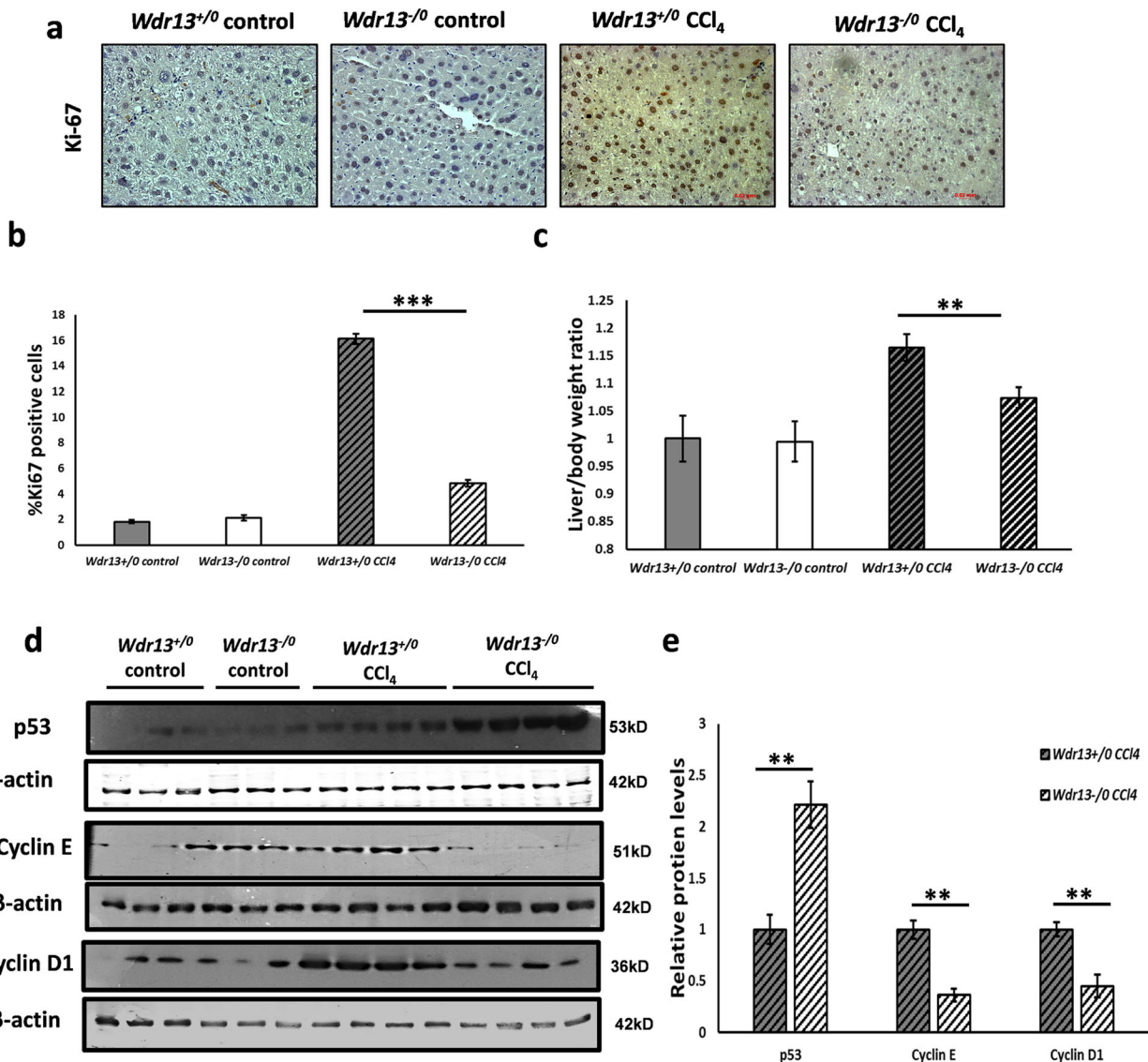
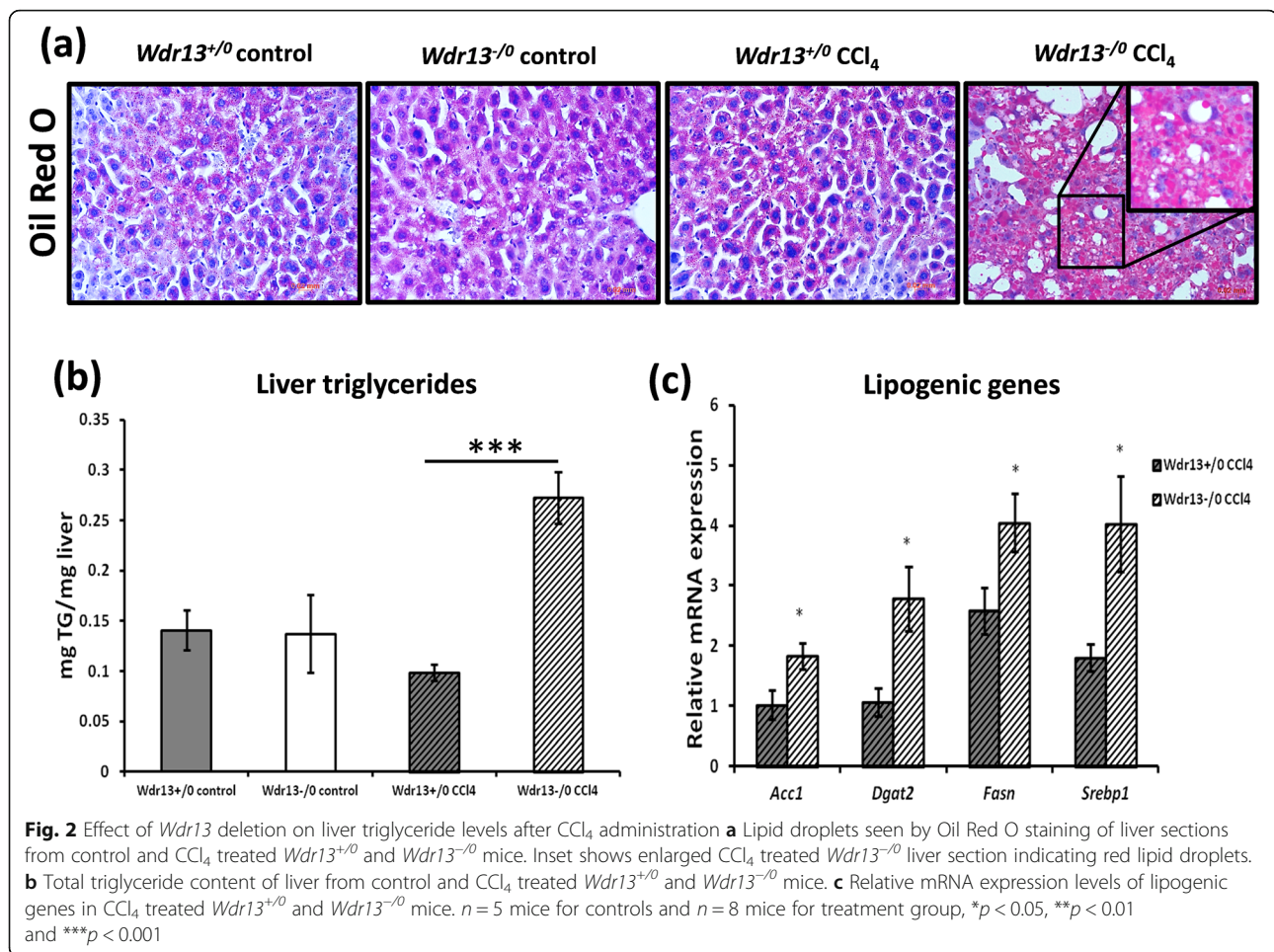


**Fig. 1** Effect of *Wdr13* deletion on liver regeneration after CCl<sub>4</sub> administration **a** Ki-67 immunostaining of liver sections from control and CCl<sub>4</sub> administered *Wdr13*<sup>+/0</sup> and *Wdr13*<sup>-/0</sup> mice. **b** Quantitative representation of Ki-67 positive cells from control and CCl<sub>4</sub> administered *Wdr13*<sup>+/0</sup> and *Wdr13*<sup>-/0</sup> liver. **c** Liver/body weight ratios of control and CCl<sub>4</sub> administered *Wdr13*<sup>+/0</sup> and *Wdr13*<sup>-/0</sup> mice. **d** p53, Cyclin E and Cyclin D1 immunoblots performed on liver proteins. All the images presented here are cropped images of full length blots for better representation and all the gels were run under similar experimental conditions. **e** Relative protein levels of p53, Cyclin E and Cyclin D1 showed in **(d)** immunoblots. ImageJ analysis of western blots was performed for quantification normalised with respective  $\beta$ -actin as loading control.  $n = 5$  mice for controls and  $n = 8$  mice for treatment group, \*\* $p < 0.01$ , \*\*\* $p < 0.001$

#### Effect of *Wdr13* deletion on serum parameters and levels of insulin responsive genes in liver after CCl<sub>4</sub> administration

Hyperglycemia and hyperinsulinemia are one of the major causes for fatty liver [19]. We analysed random serum insulin and glucose levels in control and CCl<sub>4</sub> administered *Wdr13*<sup>+/0</sup> and *Wdr13*<sup>-/0</sup> mice and observed no significant difference in these parameters (Fig. 5a,b). Obesity-induced insulin resistance is considered to be a

prime inducer of hepatosteatosis [20]. Thus, we examined insulin responsive genes in the liver, namely, *Glut4* and *Pepckc-1* by qPCR and their levels were found to be similar in CCl<sub>4</sub> administered *Wdr13*<sup>+/0</sup> and *Wdr13*<sup>-/0</sup> mice (Fig. 5d). *Cpt1*, a key gene participating in  $\beta$ -oxidation of lipids [4] that gets inhibited by hyperglycaemia and hyperinsulinemia [20] was upregulated in *Wdr13*<sup>-/0</sup> livers (Fig. 5d). These data confirmed no change in insulin sensitivity of *Wdr13*<sup>-/0</sup> mice after CCl<sub>4</sub>



administration and suggest that *Cpt1* may be upregulated as a result of hypertriglyceridemia. Lipolysis and dyslipidemia are yet major factors leading to fatty liver [4]. We thus analysed serum triglycerides and cholesterol levels in control and CCl<sub>4</sub> administered the *Wdr13*<sup>+/0</sup> and *Wdr13*<sup>-/0</sup> mice and found no significant differences (Fig. 5c). Taken together, these results indicated that the observed hepatic hypertriglyceridemia was more likely due to de novo lipogenesis in *Wdr13*<sup>-/0</sup> mice rather than due to systemic absence of *Wdr13* gene in tissues other than the liver.

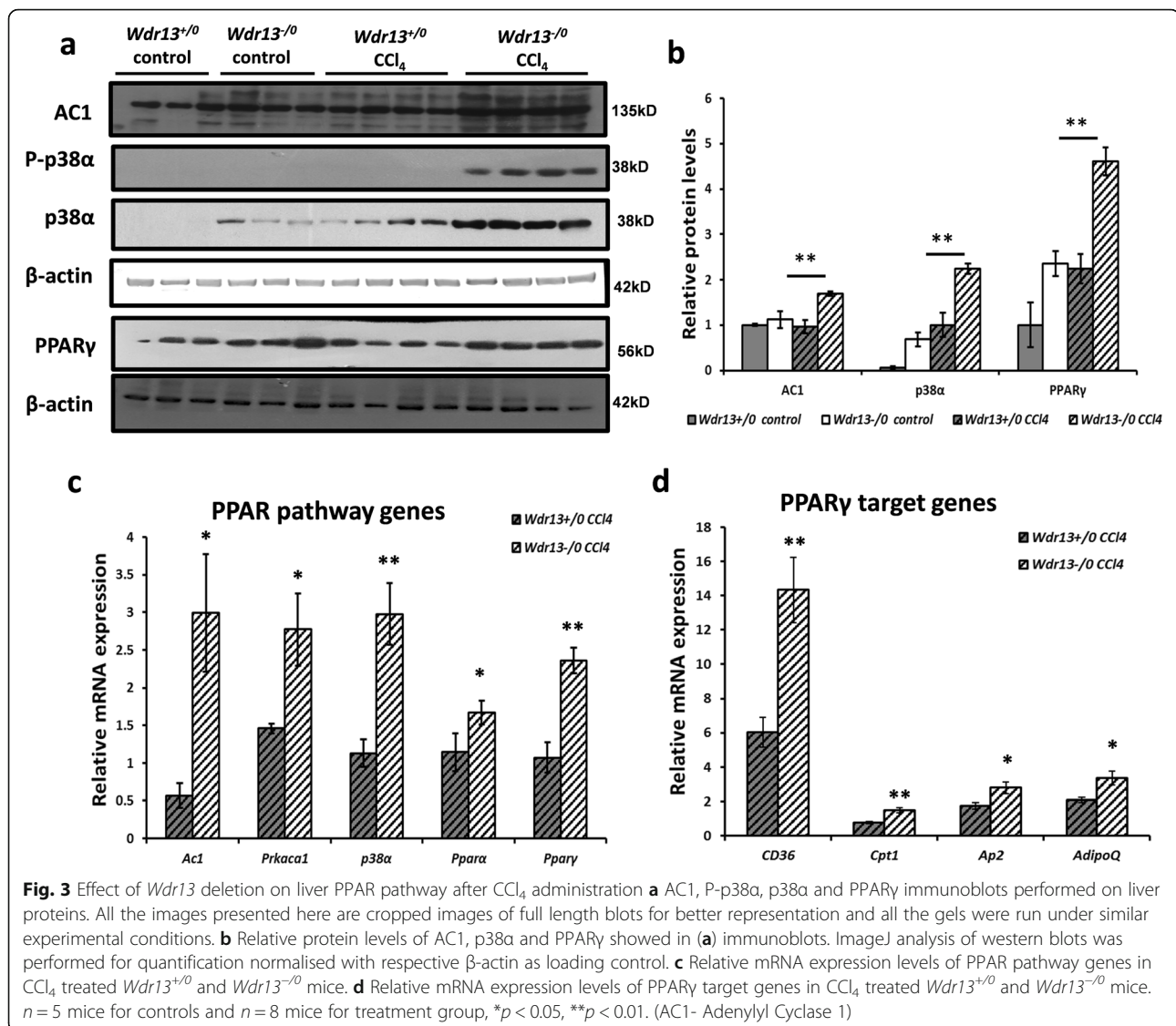
## Discussion

CCl<sub>4</sub> is an established hepatotoxin to study liver damage and regeneration [5]. It damages the liver initially via its conversion to CCl<sub>3</sub>OO\* free radical by Cytochrome P450 and later by eliciting myriad of inflammatory signals [6]. In the present study, liver damage was induced in *Wdr13*<sup>+/0</sup> and *Wdr13*<sup>-/0</sup> mice by challenging them with CCl<sub>4</sub>. The *Wdr13*<sup>-/0</sup> mice exhibited lower number of regenerating hepatocytes as compared to *Wdr13*<sup>+/0</sup> mice, thus leading to lower liver/body weight ratio. Also CCl<sub>4</sub>

was found to be more toxic on *Wdr13*<sup>-/0</sup> primary hepatocytes as compared to *Wdr13*<sup>+/0</sup> hepatocytes.

We also observed that while regenerating from chronic CCl<sub>4</sub> toxicity, *Wdr13*<sup>-/0</sup> mice accumulated higher amounts of triglycerides in liver, a condition seen in fatty liver or hepatosteatosis, seen to be via the PPAR (PPARα and PPARγ) pathway. The role of PPARs in adipose lipid metabolism and liver lipid homeostasis is well established [13, 17]. Literature reveals that liver-specific over-expression of *Pparγ* induces lipogenic gene expression, leading to hepatosteatosis [14]. Similarly, liver-specific deletion of *Pparγ* protects mice from hepatic lipid accumulation [15]. Studies also show PPARα to be a key protein involved in liver lipid metabolism [17] and its upregulation results in de novo lipogenesis and lipid chain elongation in liver [21]. The present study emphasises the role of PPAR (PPARα and PPARγ) pathway in CCl<sub>4</sub> induced hepatosteatosis in *Wdr13*<sup>-/0</sup> mice.

p38α/MAPK14 plays a pivotal role in PPAR signalling [22, 23] as it upregulates the transcriptional activity of *Pparγ* in mouse adipocytes [24] and human trophoblasts [25]. PPARs are directly linked to cAMP signalling



pathway via p38 $\alpha$ /MAPK14 [18, 23, 24, 26]. In the present study, the activation of p38 $\alpha$ /MAPK14 along with its regulatory genes- protein kinase A (PKA) and adenylyl cyclase 1 (Fig. 3), in liver of  $\text{CCl}_4$  treated *Wdr13*<sup>-/0</sup> mice, determines its role in PPAR (PPAR $\alpha$  and PPAR $\gamma$ ) pathway upregulation. This indicates that under  $\text{CCl}_4$  stress and WDR13 absence, PPAR pathway gets activated. Our previous study [11] has also indicated the role of WDR13 in regulation of *Ppar $\gamma$*  expression. Besides hepatotoxin stress, this study also reveals that the absence of WDR13 per se renders the liver susceptible to steatosis owing to the upregulated PPAR $\gamma$  and p38 $\alpha$  in the control (vehicle treated) *Wdr13*<sup>-/0</sup> mice (Fig. 3a,b). However, further investigations are required to delineate the exact role of WDR13 in the regulation of the said pathway.

Previously, we studied the liver physiology in *Lepr*<sup>db/db</sup> and *Wdr13*<sup>-/0</sup>|*Lepr*<sup>db/db</sup> double knockout mice [11]. *Lepr*<sup>db/db</sup> mice are known to have diabetes, obesity, dyslipidemia and fatty liver [27]. Onset of fatty liver in *Lepr*<sup>db/db</sup> mice is due to lipolysis and dyslipidemia resulting in heavy load of triglycerides and free-fatty acids in serum. WDR13 deletion in *Lepr*<sup>db/db</sup> mice improved adipose and pancreatic function which resulted in reduced dyslipidemia and hyperglycemia, two systemic factors contributing towards hepatosteatosis, leading to reduced serum triglycerol and free-fatty acids hence ameliorating the fatty liver phenotype. We did not study the expression of *Ppar $\gamma$*  in liver in the previous study, but other lipogenic genes were found to be upregulated in *Lepr*<sup>db/db</sup> mice in comparison to that in double knockout mice. The study confirmed that the betterment of

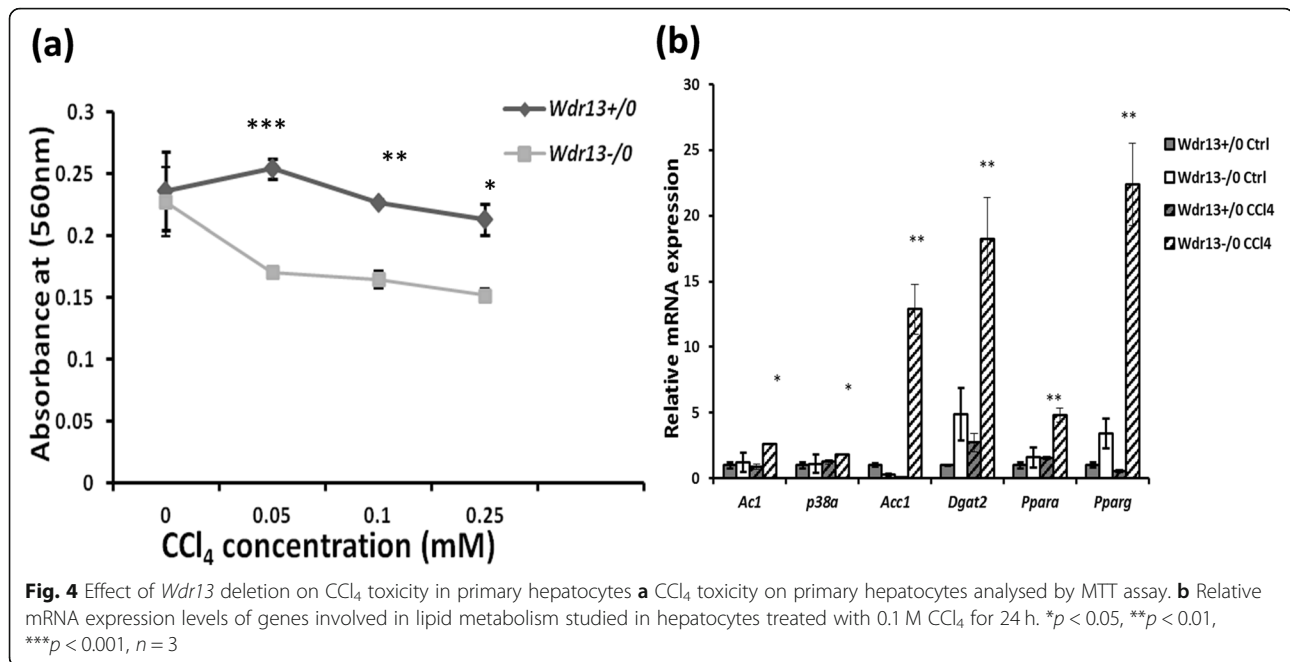


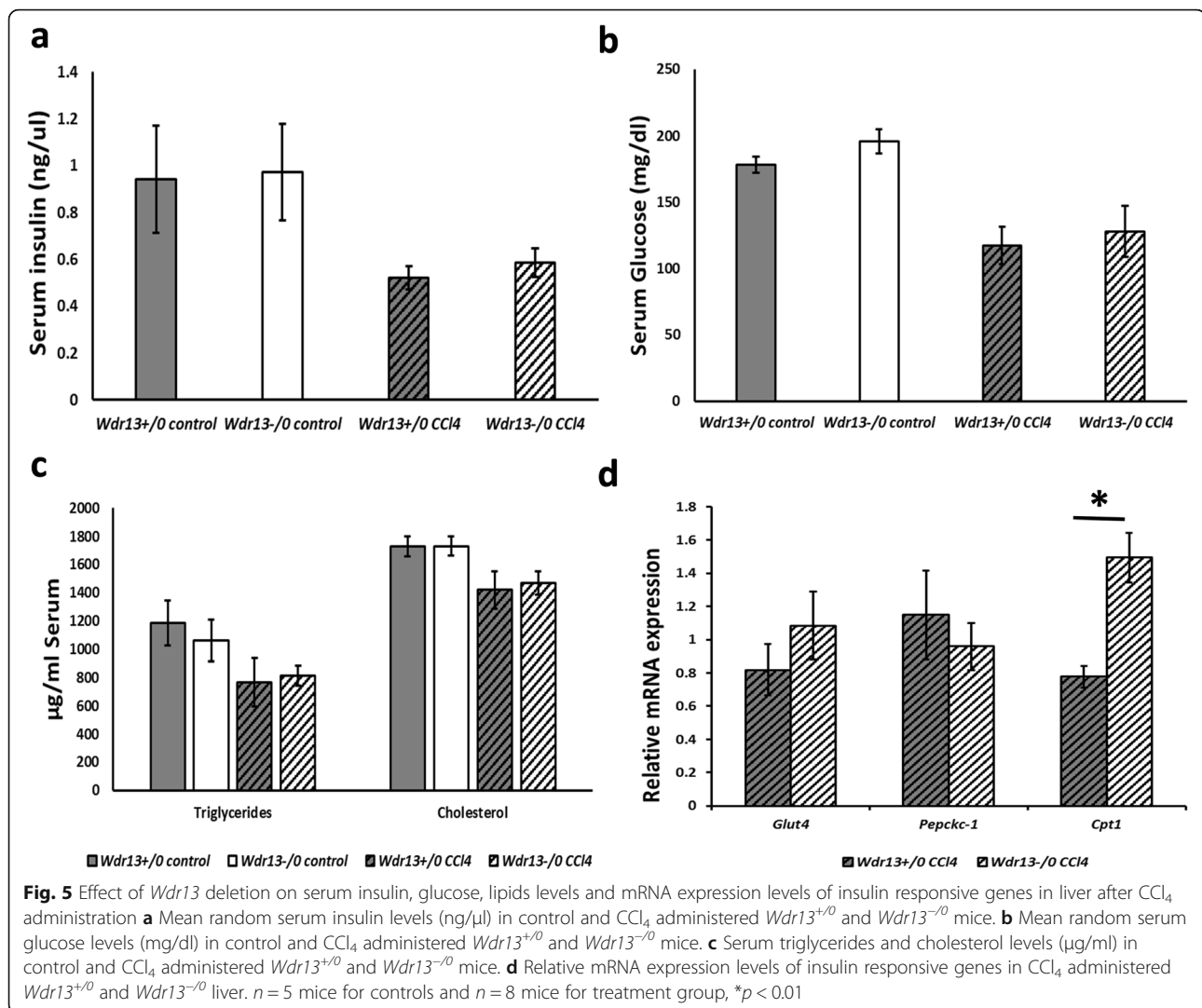
**Fig. 4** Effect of *Wdr13* deletion on CCl<sub>4</sub> toxicity in primary hepatocytes **a** CCl<sub>4</sub> toxicity on primary hepatocytes analysed by MTT assay. **b** Relative mRNA expression levels of genes involved in lipid metabolism studied in hepatocytes treated with 0.1 M CCl<sub>4</sub> for 24 h. \**p* < 0.05, \*\**p* < 0.01, \*\*\**p* < 0.001, *n* = 3

hepatic lipid profile in double knockout mice was due to improvement in the systemic factors as discussed above. Unlike the results of previous study, here we observed hepatic hypertriglyceridemia in *Wdr13*<sup>-/0</sup> mice during regeneration after CCl<sub>4</sub> intoxication. This hepatic hypertriglyceridemia is likely due to de novo lipogenesis via activated PPAR pathway. Activation of PPAR pathway is also observed in *Wdr13*<sup>-/0</sup> primary hepatocytes when treated with CCl<sub>4</sub>, which confirms that hypertriglyceridaemia seen in vivo is indeed due to the liver-specific absence of WDR13. The circulating triglycerides and cholesterol levels in *Wdr13*<sup>-/0</sup> mice were also found similar to that in *Wdr13*<sup>+/0</sup> mice, suggesting that the observed liver hypertriglyceridemia is indeed due to de novo lipogenesis and not because of systemic factors.

Hepatosteatosis is often associated with hyperglycemia and hyperinsulinemia [19]. However, in our study, there was no difference in serum insulin and glucose levels in control and CCl<sub>4</sub> administered *Wdr13*<sup>+/0</sup> and *Wdr13*<sup>-/0</sup> mice. Consistent with these data, the relative mRNA expression levels of insulin responsive genes (*Glut4* and *Pepck-c*) were also similar in the liver of CCl<sub>4</sub> administered *Wdr13*<sup>+/0</sup> and *Wdr13*<sup>-/0</sup> mice. Another insulin responsive gene, *Cpt1* which is required for mitochondrial  $\beta$ -oxidation of lipids [4] was upregulated in the liver of mutant mice. It may be noted that the expression and activity of *Cpt1* is PPAR $\alpha$  dependent [17] and the increased expression of hepatic *Cpt1* is seen in fatty liver and obesity [28]. The upregulation of *Cpt1* in *Wdr13*<sup>-/0</sup> liver may be a result of upregulated *Ppara* and liver hypertriglyceridemia.

*Wdr13*<sup>-/0</sup> livers have higher p53 and lower Cyclin D1 & E expression after CCl<sub>4</sub> administration, plausibly attributed to the elevated PPAR $\gamma$  levels. It is known that PPAR $\gamma$  activation slows the liver regeneration process [29], upregulates p53 levels (anti-proliferative gene) and downregulates cyclins in the liver [30, 31]. This seems to be an obvious reason for slower liver regeneration and lower liver/body weight ratio in *Wdr13*<sup>-/0</sup> mice.

Levels of Cyclin E were found to be higher in *Wdr13*<sup>-/0</sup> liver even without CCl<sub>4</sub> treatment (Fig. 1d). Cyclin E is crucial for G1 to S phase transition and cell cycle progression [32]. Literature suggests that activation of Cyclin E requires c-Jun which in turn is regulated by AP-1 [Activator Protein 1] [33]. Our recent data suggests that WDR13 functions via a multi protein complex c-Jun/NCoR1/HDAC3 and it acts as a transcriptional activator of AP1 target genes [34]. Besides, our previous studies have shown that the lack of WDR13 enhances the cell cycle and overexpression of the same inhibits cell proliferation [9]. It is possible that WDR13 may regulate Cyclin E expression via AP-1 and c-Jun/NCoR1/HDAC3; although presently we do not have direct evidence of it. It may be emphasised that the *Wdr13*<sup>-/0</sup> mice display hyperinsulinemia and mild obesity around 12 months of age without any evidence of fatty liver phenotype [9]. To avoid confounding effects of the absence of WDR13 per se on metabolism and the toxic effects of CCl<sub>4</sub>, the present study was conducted at the age of 8–10 weeks old animals when there is no onset of hyperinsulinemia and obesity. Fatty liver condition



in mice has been reported upon treatment with  $\text{CCl}_4$  along with high fat diet [35] via upregulation of PPARy in the liver [36]. In this study we observed fatty liver phenotype in *Wdr13*<sup>-/0</sup> mice on  $\text{CCl}_4$  treatment alone, owing to upregulation of PPAR pathway. Thus in our opinion, this study introduces WDR13 as a molecular factor, the absence of which predisposes mice to hepatosteatosis in the presence of  $\text{CCl}_4$  (without the requirement of high fat diet).

## Conclusions

In the present study we report that the *Wdr13*<sup>-/0</sup> mice are more susceptible to  $\text{CCl}_4$ - induced hepatotoxicity as compared to their wild type counterparts. Also the *Wdr13*<sup>-/0</sup> mice exhibit liver hypertriglyceridemia due to de novo lipogenesis, during the regeneration phase after  $\text{CCl}_4$  toxicity. PPAR pathway upregulation in liver has a key role in the observed phenotypes of  $\text{CCl}_4$

administered *Wdr13*<sup>-/0</sup> mice.  $\text{CCl}_4$  is an established hepatotoxin to study hepatic damage, fibrosis and regeneration in murine models, but fatty liver has never been reported in exclusive  $\text{CCl}_4$  toxicity in mice. *Wdr13*<sup>+/0</sup> mice manage the  $\text{CCl}_4$  challenge and do not allow PPAR pathway to get upregulated. This study indicates that under  $\text{CCl}_4$  stress PPARy gets overexpressed in the absence of WDR13 suggesting WDR13 may have a role in regulation of PPARy expression, as also seen in our previous study [11]. We want to highlight the fact that absence of WDR13 per se does not induce de novo lipogenesis and fatty liver but when these mutant mice are subjected to  $\text{CCl}_4$  stress, liver hypertriglyceridemia is observed via upregulation of PPAR pathway. However, at present we do not understand how the absence of WDR13 activates the PPAR pathway. Further experiments are required to elaborate the mode of action of WDR13 in regulation of PPARs.

## Methods/experimental

### Animals

Institutional Animal Ethics Committee (IAEC) of CSIR-CCMB, Hyderabad, India (Animal trial registration number- 20/1999/CPCSEA dated 10/3/99) approved the animal experiments and the experiments were performed under IAEC guidelines. 8–10 week old *Wdr13* knockout (*Wdr13*<sup>-0</sup>) CD1 male mice [PCR genotyped as described earlier [9]] along with their wild type (*Wdr13*<sup>+0</sup>) littermates were used in the study. Mice were housed at 22–25 °C temperature with 12 h light-dark cycle. All the mice were fed standard chow for entire experimental duration ad libitum.

### CCl<sub>4</sub> administration

Mice were injected (intraperitoneally) with CCl<sub>4</sub> (10% v/v dissolved in olive oil, 2 ml/kg body weight), twice a week for 8 consecutive weeks. Controls were injected with vehicle (olive oil) similarly. After the last injection, mice were given a 10-days of recovery period and then sacrificed for physiological and molecular analyses.

### Liver/body weight ratio

Mice were weighed before sacrificing. Whole liver was carefully excised out and weighed. Ratio of respective liver weight to body weight was taken and graph was plotted.

### Histological analyses

Liver was fixed in 4% paraformaldehyde overnight and then embedded in paraffin wax. Four micrometers sections of livers were mounted on positively charged slides (Fischer scientific) and hematoxylin-eosin staining was performed for visualizing tissue morphology. Sirius Red staining was performed to study collagen deposition. For Oil Red O staining, the livers were stored in tissue freezing medium (Sigma-Aldrich) and cryosections of 10 μm were prepared. These sections were stained with 0.5% Oil Red O (MPBio, 0215598483) [prepared in isopropanol] and counterstained with Gill's hematoxylin. To evaluate the number of actively dividing cells in the liver, Ki-67 immunostaining was performed according to manufacturer's guidelines (BD Biosciences DAB substrate kit Cat.-550,880, Ki-67 antibody- Millipore- AB9260). Ki-67 positive cells were counted manually (3 frames per section) from 5 different animals.

### Serum collection and analyses

Five hundred microliters of blood was drawn from the mice orbital sinus and left to clot in a slanting position at room temperature for 2 h for serum collection. The serum was collected by centrifugation at 10,000 g for 10 min. Liver function tests- SGOT (Serum glutamic oxaloacetic transaminase) and SGPT (Serum glutamic-pyruvic

transaminase) were performed as per the manufacturer's instructions (Coral Clinical Systems). Serum glucose was tested using Accu-Chek® Active Glucometer (model number: HM100005). Level of serum insulin was determined using insulin ELISA kit (Millipore-EZMRI-13 K).

### TBARS assay

The assay was performed following spectrophotometric measurement of colour generated by the reaction of MDA (Malondialdehyde) with thiobarbituric acid (TBA) as described earlier [37]. Briefly, 50 mg of liver was homogenized in PBS. The supernatant was collected after centrifuging the homogenate at 10,000 g. Five hundred microliters of trichloroacetic acid (10%) was added to 100 μl of supernatant and heated at 95 °C for 15 min. The mixture was cooled to room temperature and centrifuged at 3000 g for 10 min. Two hundred microliters of TBA (0.67% in 1 M NaOH) was added to 400 μl of the supernatant from the previous step. This mixture was then heated at 95 °C for 15 min. After cooling the samples to room temperature, 200 μl of the same was taken in a microtitre plate and absorbance was recorded at 532 nm. MDA concentration was determined using the absorbance coefficient of the TBA-MDA complex ( $\epsilon = 1.56 \times 10^5 \text{ cm}^{-1} \cdot \text{M}^{-1}$ ).

### Liver triglycerides

Total lipid from liver was extracted using Folch's method [38]. Briefly, 50 mg of liver sample was homogenized in chloroform:methanol (2:1) mixture. The homogenate was vigorously agitated for 15–20 min and centrifuged at 12,000 g. The supernatant was washed by adding 0.2 volume water and gentle mixing. The upper phase was removed and the lower one was vacuum dried. One hundred microliters of ethanol was added to the dried tube and kept at 4 °C overnight for dissolving the deposited fat. Triglyceride estimation was done using an assay kit (Coral Clinical Systems).

### Western blotting

Fifty milligrams of liver sample was homogenised in lysis buffer [50 mM Tris pH 8.0, 150 mM NaCl, 0.1% SDS, 1% Na-deoxycholate, 1% Triton X100, 1X protease inhibitor cocktail (Roche 11,873,580,001)] and supernatant was collected after centrifuging at 10,000 g. After protein estimation, 50 μg of the lysate was run on SDS-PAGE and transferred to PVDF membrane. Membrane was probed with protein specific antibodies-  $\beta$ -actin (1:1000 dilution, Santacruz sc-47,778), p53 (1:500 dilution, Santacruz sc-6243), Cyclin D1 (1:500, Santacruz sc-246), Cyclin E (1:500, Santacruz sc-481), AC1 (1:500, Novusbio NBP1-19628), p38 $\alpha$  (1:500, Santacruz sc-535), P-p38 $\alpha$  (1:500 dilution, Santacruz sc-101,759) and PPAR $\gamma$  (1:500 dilution, Cell Signaling 2435S). For stripping the PVDF

membrane, it was incubated in stripping buffer (0.1 M  $\beta$ -mercaptoethanol, 2% SDS, 62.5 mM Tris-HCl, pH 6.7) at 50 °C for 30 min. The blot were washed thoroughly and reprobed with different primary antibodies.

### RNA isolation and real-time PCR

Fifty milligrams of liver sample was taken in 1 ml RNAiso (Takara Cat.-9108/9109) and RNA was isolated

according to the manufacturer's guidelines. cDNA was synthesized using ImProm-II Reverse Transcription System (Promega- A3800). Quantitative real-time PCR (qPCR) was done using Ex Taq SYBR Green (Takara-RR820A), gene specific primers (Table 1) and  $\beta$ -actin for normalisation.

**Table 1** Primers used for qPCR

Gene	Sequence (5'---- 3')
<i>Ac1</i>	GTCACCTTCGTGCTCCTATGCC TTCACACCAAAGAAGAGCAGG
<i>p38a</i>	GGCTCGGCACACTGATGAT TGGGGTTCCAACGAGTCTTAAA
<i>Prkaca1</i>	GTCAAAGCCGACCAATGATA CGTACACGCAAATAATAGGGGTT
<i>Ppara</i>	AGAGCCCCATCTGCTCTCTC ACTGGTAGTCTGCAAAACAAA
<i>Cd36</i>	CAGCAAGGCCAGATATCACA GAGCTATGCAGCATGGAACA
<i>Il-1 <math>\beta</math></i>	AGGCCACAGGTATTTTGTGCG GCCATCCTCTGTGACTCAT
<i>Il10</i>	TGGCCAGAAATCAAGGAGC CAGCAGACTCAATACACT
<i>Ifny</i>	AGGTCAACAACCCACAGGTC ATCAGCAGCGACTCCTTTTC
<i>Tnfa</i>	GAAACACACGAGACGCTGAA CAGTCTGGGAAGCTCTGAGG
<i>Acc1</i>	TGGATCCGCTTACAGAGAGACT GCCGGAGCATCTCATTCG
<i>Dgat2</i>	GCACAGAGGCCACAGAAGTG CCCTCAACACAGGCATCG
<i>Ppar<math>\gamma</math></i>	CGGTTTCAGAAGTGCCTTG GGTTCAGCTGGTCGATATCAC
<i>Pepck-1</i>	GTCAACACCACCTCCCTTA CCCTAGCCTGTCTCTGTGC
<i>Sreb1c</i>	GGAGCCATGGATTGCACATT GCTTCCAGAGAGGAGCCAG
<i>Fasn</i>	GCCTGGACTCGCTCATGG TGAAGTTTCCGACGCGTG
$\beta$ -actin	ATGCTCCCCGGGCTGTAT CATAGGAGTCCTTCTGACCCAT
<i>Il6</i>	GAAGTAGGGAAGGCCGTGG CTGCAAGAGACTTCCATCCAGT
<i>Glut4</i>	AACGAGCTGGACGACGGACA TTGCCCTCAGTCATTCTCA
<i>Emr1</i>	TTTCTCGCCTGCTTCTTC CCCCGTCTCTGTATTCAACC
<i>Ap2</i>	TGGAAGCTTGTCTCCAGTGA ATTTCATCCAGGCCTCTT
<i>Adipoq</i>	CCGCTTATGTGTATCGCTCA GTAGAGTCCCGAATGTTGC
<i>Cpt1</i>	GACCCTAGACACCAGTGGCCG GAGAGGACCTTGACCATAGCC

### Primary hepatocyte isolation and culture

Isolation of primary hepatocytes was done with the double perfusion collagenase method as described earlier [39]. Trypan blue staining was used for cell viability determination. Cells were seeded on collagen coated 6-well plates ( $6 \times 10^5$  viable cells/well). The cells were grown in RPMI media (50  $\mu$ g/ml penicillin and streptomycin, 10% FBS) in 5% CO<sub>2</sub> incubator at 37 °C. After 24 h of incubation, fresh RPMI media comprising 100  $\mu$ M CCl<sub>4</sub> (dissolved in DMSO) was added to specific wells. After 24 h of CCl<sub>4</sub> administration, the hepatocytes were harvested and total RNA was isolated for qPCR analyses.

### CCl<sub>4</sub> toxicity assay on hepatocytes-

This assay was done using MTT [3-(4,5-Dimethylthiazol-2-yl)-2,5-Diphenyltetrazolium Bromide] colorimetric assay for cellular growth and survival, as described earlier [40]. Briefly, 1000 viable hepatocytes were counted and seeded in triplicates in 96-well plate (coated with collagen) and incubated in RPMI media for 4 h for attachment. Fresh media with different concentrations of CCl<sub>4</sub> (0–0.25 mM dissolved in DMSO) was added to the specific wells and incubated for 24 h at 37 °C and 5% CO<sub>2</sub>. After 24 h, the wells were washed with PBS and cells were incubated with 0.8 mg/ml of MTT dissolved in serum free RPMI media for 4 h. After incubation, the wells were again washed with PBS and 200  $\mu$ l of DMSO was added to each well. After a gentle shaking for 10 min, absorbance was taken at 560 nm.

### Statistical analyses

All the graphs were plotted using MS Excel worksheet. Single factor ANOVA and two-tailed unpaired student's t-test were used for statistical analyses. Graphs represent mean  $\pm$  SEM.

### Supplementary information

The online version contains supplementary material available at <https://doi.org/10.1186/s42826-020-00076-8>.

Additional file 1

### Abbreviations

WDR13: WD repeat domain 13; CCl<sub>4</sub>: Carbon tetrachloride; H&E: Hematoxylin and Eosin; TBARS: Thiobarbituric acid reactive substances; SGOT: Serum glutamic oxaloacetic transaminase; SGPT: Serum glutamic-pyruvic transaminase

### Acknowledgements

We thank Mr. Avinash T Raj for histology and Dr. Sesikeran for histological assessments. We acknowledge the Council of Scientific and Industrial Research (CSIR), New Delhi, India for financial support to Mr. Arun Prakash Mishra. The experiments were conducted in Dr. Satish Kumar's laboratory.

### Authors' contributions

APM, CGS and ABS conceived the idea, designed experiments and wrote the manuscript. APM, KY and BJL performed the experiments. The author(s) read and approved the final manuscript.

### Funding

No separate funding was allotted to this study.

### Availability of data and materials

Raw data will be available on request.

### Competing interests

Authors declare no conflict of interest.

Received: 1 September 2020 Accepted: 8 November 2020

Published online: 13 November 2020

### References

- Neff GW, Duncan CW, Schiff ER. The current economic burden of cirrhosis. *Gastroenterol Hepatol (N Y)*. 2011;7(10):661–71.
- Alhonen L, Räsänen T-L, Sinervirta R, Parkkinen J, Korhonen V-P, Pietilä M, et al. Polyamines are required for the initiation of rat liver regeneration. *Biochem J*. 2002;362(Pt 1):149–53.
- Bataller R, Brenner DA. Liver fibrosis. *J Clin Invest*. 2005;115(2):209–18.
- Reddy JK, Rao MS. Lipid metabolism and liver inflammation. II. Fatty liver disease and fatty acid oxidation. *Am J Physiol Gastrointest Liver Physiol*. 2006;290(5):G852–8.
- Rahman TM, Hodgson HJ. Animal models of acute hepatic failure. *Int J Exp Pathol*. 2000;81(2):145–57.
- Weber LWD, Boll M, Stampfl A. Hepatotoxicity and mechanism of action of Haloalkanes: carbon tetrachloride as a toxicological model. *Crit Rev Toxicol*. 2003;33(2):105–36.
- Krizhanovsky V, Yon M, Dickens RA, Hearn S, Simon J, Miething C, et al. Senescence of activated stellate cells limits liver fibrosis. *Cell*. 2008;134(4):657–67.
- Singh BN, Suresh A, UmaPrasad G, Subramanian S, Sultana M, Goel S, et al. A highly conserved human gene encoding a novel member of WD-repeat family of proteins (WDR13). *Genomics*. 2003;81(3):315–28.
- Singh VP, Lakshmi BJ, Singh S, Shah V, Goel S, Sarathi DP, et al. Lack of Wdr13 gene in mice leads to enhanced pancreatic beta cell proliferation, hyperinsulinemia and mild obesity. *PLoS One*. 2012;7(6):1–10.
- Mishra AP, Yedella K, Lakshmi JB, Siva AB. Wdr13 and streptozotocin-induced diabetes. *Nutr Diabetes*. 2018;8(1):57.
- Singh VP, Gurunathan C, Singh S, Singh B, Lakshmi BJ, Mishra AP, et al. Genetic deletion of Wdr13 improves the metabolic phenotype of Lepr db/db mice by modulating AP1 and PPAR $\gamma$  target genes. *Diabetologia*. 2015;58(2):384–92.
- Ruch RJ, Klaunig JE, Schultz NE. Mechanisms of chloroform and carbon tetrachloride toxicity in primary cultured mouse hepatocytes. *Environ Health Perspect*. 1986;69(11):301–5.
- Ables GP. Update on Ppar and nonalcoholic fatty liver disease. *PPAR Res*. 2012;2012:1–5.
- Yu S. Adipocyte-specific gene expression and Adipogenic Steatosis in the mouse liver due to peroxisome proliferator-activated receptor gamma 1 (PPAR $\gamma$ 1) overexpression. *J Biol Chem*. 2002;278(11):498–505.
- Morán-Salvador E, López-Parra M, García-Alonso V, Titos E, Martínez-Clemente M, González-Pérez A, et al. Role for PPAR $\gamma$  in obesity-induced hepatic steatosis as determined by hepatocyte- and macrophage-specific conditional knockouts. *FASEB J*. 2011;25(8):2538–50.
- Inoue M, Ohtake T, Motomura W, Takahashi N, Hosoki Y, Miyoshi S, et al. Increased expression of PPAR $\gamma$  in high fat diet-induced liver steatosis in mice. *Biochem Biophys Res Commun*. 2005;336(1):215–22.
- Kersten S. Integrated physiology and systems biology of PPAR $\alpha$ . *Mol Metab*. 2014;3(4):354–71.
- Lazennec G, Canaple L, Saugy D, Wahli W. Activation of peroxisome proliferator-activated receptors (PPARs) by their ligands and protein kinase a activators. *Mol Endocrinol*. 2000;14(12):1962–75.
- Perry RJ, Samuel VT, Petersen KF, Shulman GI. The role of hepatic lipids in hepatic insulin resistance and type 2 diabetes. *Nature*. 2014;510(7503):84–91.
- Rasmussen BB, Holmbäck UC, Volpi E, Morio-Liondore B, Paddon-Jones D, Wolfe RR. Malonyl coenzyme a and the regulation of functional carnitine palmitoyltransferase-1 activity and fat oxidation in human skeletal muscle. *J Clin Invest*. 2002;110(11):1687–93.
- Oosterveer MH, Grefhorst A, van Dijk TH, Havinga R, Stals B, Kuipers F, et al. Fenofibrate simultaneously induces hepatic fatty acid oxidation, synthesis, and elongation in mice. *J Biol Chem*. 2009;284(49):34036–44.
- Barger PM. p38 mitogen-activated protein kinase activates peroxisome proliferator-activated receptor alpha. A potential role in the cardiac metabolic stress response. *J Biol Chem*. 2001;276(48):44495–501.
- Kelly DP. The pleiotropic nature of the vascular PPAR gene regulatory pathway. *Circ Res*. 2001;89:935–7.
- Hata K, Nishimura R, Ikeda F, Yamashita K, Matsubara T, Nokubi T, et al. Differential Roles of Smad1 and p38 Kinase in Regulation of Peroxisome Proliferator-activating Receptor  $\gamma$  during Bone Morphogenetic Protein 2-induced Adipogenesis. Heldin C-H, editor. *Mol Biol Cell*. 2003;14:545–55.
- Schild RL, Sonnenberg-Hirche CM, Schaiff WT, Bildirici I, Nelson DM, Sadovsky Y. The kinase p38 regulates peroxisome proliferator activated receptor- $\gamma$  in human Trophoblasts. *Placenta*. 2006;27(2–3):191–9.
- Wang S, Awad KS, Elinoff JM, Dougherty EJ, Ferreyra GA, Wang JY, et al. G Protein-Coupled Receptor 40 (GPR40) and Peroxisome Proliferator-Activated Receptor  $\gamma$  (PPAR $\gamma$ ): An Integrated Two-Receptor Signaling Pathway. *J Biol Chem*. 2015;40(32):jbc.M115.638924.
- Sharma K, McCue P, Dunn SR. Diabetic kidney disease in the db/db mouse. *Am J Physiol Renal Physiol*. 2003;284(6):F1138–44.
- Begriffe K, Massart J, Robin MA, Bonnet F, Fromenty B. Mitochondrial adaptations and dysfunctions in nonalcoholic fatty liver disease. *Hepatology*. 2013;58(4):1497–507.
- Yamamoto Y, Ono T, Dhar DK, Yamanoi A, Tachibana M, Tanaka T, et al. Role of peroxisome proliferator-activated receptor-gamma (PPAR $\gamma$ ) during liver regeneration in rats. *J Gastroenterol Hepatol*. 2008;23(6):930–7.
- Bonofiglio D, Aquila S, Catalano S, Gabriele S, Belmonte M, Middea E, et al. Peroxisome proliferator-activated receptor- $\gamma$  activates p53 gene promoter binding to the nuclear factor- $\kappa$ B sequence in human MCF7 breast cancer cells. *Mol Endocrinol*. 2006;20(12):3083–92.
- Nagamine M, Okumura T, Tanno S, Sawamukai M, Motomura W, Takahashi N, et al. PPAR gamma ligand-induced apoptosis through a p53-dependent mechanism in human gastric cancer cells. *Cancer Sci*. 2003;94(4):338–43.
- Ohtsubo M, Theodoras AM, Schumacher J, Roberts JM, Pagano M. Human cyclin E, a nuclear protein essential for the G1-to-S phase transition. *Mol Cell Biol*. 1995;15(5):2612–24.
- Hess J, Angel P, Schorpp-Kistner M. AP-1 subunits: quarrel and harmony among siblings. *J Cell Sci*. 2004;117(25):5965–73.
- Singh VP, Katta S, Kumar S. WD-repeat protein WDR13 is a novel transcriptional regulator of c-Jun and modulates intestinal homeostasis in mice. *BMC Cancer*. 2017;17(1):148.
- Kubota N, Kado S, Kano M, Masuoka N, Nagata Y, Kobayashi T, et al. A high-fat diet and multiple administration of carbon tetrachloride induces liver injury and pathological features associated with non-alcoholic steatohepatitis in mice. *Clin Exp Pharmacol Physiol*. 2013;40(7):422–30.
- Allman M, Gaskin L, Rivera C. a. CCl4-induced hepatic injury in mice fed a Western diet is associated with blunted healing. *J Gastroenterol Hepatol*. 2010;25(3):635–43.
- Draper HH, Squires EJ, Mahmoodi H, Wu J, Agarwal S, Hadley M. A comparative evaluation of thiobarbituric acid methods for the determination of malondialdehyde in biological materials. *Free Radic Biol Med*. 1993;15(4):353–63.
- Folch J, Lees M, Stanley GHS. A simple method for the isolation and purification of total lipids from animal tissues. *J Biol Chem*. 1957;226(1):497–509.
- Holl D, Kuckenberger P, Woynecki T, Egert A, Becker A, Huss S, et al. Transgenic overexpression of Tcfap2c/AP-2gamma results in liver failure and intestinal dysplasia. *PLoS One*. 2011;6(7):e22034.
- Mosmann T. Rapid colorimetric assay for cellular growth and survival: application to proliferation and cytotoxicity assays. *J Immunol Methods*. 1983;65(1):55–63.

### Publisher's Note

Springer Nature remains neutral with regard to jurisdictional claims in published maps and institutional affiliations.